Desalination and Water Treatment
www.deswater.com

doi: 10.5004/dwt.2017.0433

60 (2017) 319–328
January

Application of nickel oxide nanoparticles as reusable sorbent for the removal of lead ions from contaminated water

Farideh Rostamkhani[a], Hassan Karami[a,b,*], Anahita Ghasemi[a]

[a]*Nano Research Laboratory, Department of Chemistry, Payame Noor University, Abhar, Iran, emails: karami_h@yahoo.com (H. Karami), Rostamkhani.shimi@gmail.com (F. Rostamkhani), anaghasemi302@yahoo.com (A. Ghasemi)*
[b]*Department of Chemistry, Payame Noor University, PO Box 19395-3697, Tehran, Iran, email: karami_h@yahoo.com*

Received 18 April 2016; Accepted 9 July 2016

ABSTRACT

In this study, NiO nanopowder (NONP) is prepared using a sol-gel method based on polyvinyl alcohol (PVA) as gel precursor agent. The produced NONP is characterized by TGA, FTIR, TEM, SEM, DLS and XRD. The results show that the synthesized sample consists of uniform nanoparticles in the range of 10–25 nm with an average diameter of 15 and 20 nm based on the TEM micrograph and DLS results, respectively. The synthesized NONP is used as a new and efficient nanosorbent for the removal of heavy metal cations such as lead ions from solutions with high concentrations of pollution. Kinetic and equilibrium studies showed that the experimental data of Pb(II) ions were best described by pseudo-second-order and Langmuir isotherm models. The obtained results showed that the quantitative removal of Pb^{2+} ions can be performed under the optimized conditions, including 100 μg ml^{-1} initial concentration of lead ions with a pH of 5, 2.0 mg ml^{-1} sorbent dosage and contact time of 1 h in room temperature. The maximum sorption capacity for Pb (II) on NONP is found to reach up to 50.7 mg g^{-1}. The experimental results indicate that the NONP can not only be used as a high performance nanosorbent for the removal of lead ions but also reused frequently without significant loss in sorption efficiency for five times.

Keywords: NiO nanopowder; Sol-gel method; Contaminated water; Lead ion removal

1. Introduction

The contamination of waters and wastewaters by toxic heavy metals is a worldwide environmental problem. These toxic metal ions such as Pb, Cd, Hg and As commonly exist in waste streams from mining operations, metal plating facilities, batteries facilities, and etc. [1]. In higher doses, they can detrimentally effect on the health of most living organisms [2]. Nowadays, numerous methods have been proposed for the efficient removal of heavy metal ions from waters, such as chemical precipitation [3,4], ion exchange [5,6], adsorption [7–10], membrane filtration and electrochemical technologies [11,12]. Among these techniques, adsorption offers flexibility in design and operation, and also the adsorbents can be regenerated by suitable desorption processes for multiple use [13]. Major of desorption processes are of low maintenance cost, high efficiency, and ease of operation [14]. Many types of sorbents, including activated carbon, oxide minerals, polymer fibers, resins, low-cost materials and biosorbents, have been used to adsorb or to remove Pb(II) ions from various aqueous solutions [15–22]. In the recent years, an increasing attention has been given on the synthesis and application of nanomaterials as adsorbents or catalysts to remove toxic and harmful substances from water. Recently, NiO has been studied as a suitable absorbent, for the removal of heavy metals because of its simplicity, high efficiency, high adsorption capacity and regeneration of sorbent. The application of nickel oxide nanoparticles for water treatment has been

* Corresponding author.

reported by researchers for the treatment Cd (II), Co (II) and Zn (II) [23], Pb (II) and Cd (II) [24], and etc.

In the present study, nickel oxide nanoparticles were initially synthesized by the sol-gel method based on polyvinyl alcohol (PVA) as gel making agent. In the sol-gel method for the synthesis of nanoparticles of metal oxides, often an organic alkoxide such as PVA as gel making agent is used. Organic alkoxide can often have chemical interaction of metal cations. Alkoxide containing functional groups of the type R-O during the interaction with metal cations can be converted to M-OR. This interaction occurs in the cage of sol. When the sol is converted into the gel, the place of this metal species fixed within the gel network. With controlling features of the network and the concentration of the target species, the particle size and the morphology of yield can be controlled [25]. In this synthesis technique, NiO nanoparticles have larger surface area and a great desire to interact with other substances.

The synthesized NiO nanopowder (NONP) was characterized by different techniques. Finally, the synthesized NONP was used as a new sorbent for the removal of lead ions from solutions with high concentrations of pollution. The effect of all sorption parameters was investigated and optimized by the "one at a time" method.

2. Experimental

2.1. Materials

Fe $(NO_3)_2$, Pb $(NO_3)_2$. H_2O, Zn $(NO_3)_2.6H_2O$, $NiSO_4$, $CuSO_4.5H_2O$, Mn $(NO_3)_2.4H_2O$, $NaNO_3$, Al_2 $(SO_4)_3.18H_20$, $MgSO_4$, and HNO_3 as the chemicals in analytical grade were purchased from Merck and used without further purification. PVA with K_{value} of 72,000 were obtained from Merck. Double-distilled water was used in all experiments.

2.2. Instrumentals

The synthesized NONP was characterized by scanning electron microscopy (SEM; XL 30, Philips), X-ray diffraction (XRD; Shimadzu 6000 with copper K_α incident radiation) and transmission electron microscopy (TEM; ZEISS EM900). Fourier transform infrared spectroscopy (FTIR; Thermo Scientific Nicolet IS 10) was used to study the mechanism of lead ions adsorption on NONP. Size distribution diagram of the sample was obtained by DLS (Malvern Instruments Ltd, Zetasizer Ver. 6.32). Flame atomic absobtion spectrophotometer (GBC, Sense AA, Austria) was used to demine the residual concentrations of the heavy metal ions. A 2,500 rpm centrifuge (Wagtech Co.C257-176) and also cellulose acetate membrane (0.45 μm micro pore) were used to separate the NONP from solution in adsorption and desorption studies, respectively.

2.3. Experimental procedures

2.3.1. Synthesis of NONP

NONP were synthesized by the sol-gel pyrolysis method based on PVA as gel precursor. In practice, in a 250 ml beaker, 48 ml water was added. Then, 2 g anhydrous nickel sulfate was added and the mixture was well stirred by using a magnetic stirrer at 400 rpm while the baker was slightly heated until nickel salt to be dissolved. 48 ml ethanol 70% and 2 g PVA gradually added to the solution while the mixture is stirred and heated up to 70°C to obtain a homogeneous soil. The obtained soil was heated up to 90°C to evaporate the major part of the solvent and to form a uniform high viscous gel. The obtained gel was pyrolized at 450°C for 3 h. During pyrolysis, the nickel sulfate molecules were slowly calcinated to form NiO in nanopowder form.

2.3.2. Adsorption experiments

After synthesis of NONP, the adsorption ability of NONP for some heavy metal ions was examined. In this step, 100 mg NONP was added to 50 ml of each metal ion (Pb^{2+}, Cu^{2+}, Zn^{2+}, Fe^{2+}, Mn^{2+}, and Mg^{2+}) solution with the same concentration of 20 ppm with pH 4. The mixtures were stirred for 30 min at 400 rpm and then, the adsorbent nanoparticles separated from the solution by centrifuging. The residual concentrations of the proposed ions were determined by the flame atomic absorption spectroscopy. Among the examined metal ions, lead ions can be quantitavely removed by NONP from water. Therefore, in next steps, the experimental conditions for the removal of lead ions were fully studied. The effect of pH was investigated at 25°C and initial concentration 100 μg ml^{-1}. pH adjustments were done by using 0.1 M HNO_3 solution and 0.1 M NaOH. The optimization experimental studies were conducted at different pHs of 2–7, adsorbent dosage of 0.2–15 mg ml^{-1}, initial lead ion concentration of 100–1,000 μg ml^{-1}, mixing (contact) times of 10–90 min, solution temperatures of 5°C–70°C and different sample volume of 25–500 ml. In all experiments, the removal efficiency was calculated by the Eq. (1):

$$\text{Removal efficiency (\%)} = \frac{C_i - C_f}{C_i} \times 100 \quad (1)$$

where C_i (μg ml^{-1}) and C_f (μg ml^{-1}) are the initial and final concentrations of lead ions before and after mixing with NONP, respectively. The equilibrium adsorption capacity (q_e (mg g^{-1})) of lead ions was calculated using the mass balance Eq. (2):

$$q_e = \frac{(C_i - C_e)}{m} V \quad (2)$$

where C_e (μg ml^{-1}) is the equilibrium concentration of metal ions, V (ml) is the sample volume, and m (mg) is the amount of NONP.

2.4. Desorption studies

Regeneration is an important factor for advanced adsorbents. Better desorption substantially decreases the total costs associated with removal, especially when high costs. In the regeneration study, initial studies showed that acidic solvent was quite favorable for regeneration of NONP. Among different acids, HNO_3 was selected as the most suitable solvent for the regeneration of NONP. To investigate the regeneration operation of the NiO, some 50 ml solution with a constant

concentration of lead ion (100 μg ml^{-1}) were prepared and constant amount of adsorbent (2.0 mg ml^{-1}) was added. The mixtures were stirred with a speed of 400 rpm until the system reached equilibrium. The mixture was filtered by a 0.45 μm membrane and then, the loaded NiO was treated with different volumes of 3 M HNO_3 solution. The recovered concentration of lead ions in the eluted solutions was determined. In the next step, the effect of HNO_3 concentration in the range of 1–5 M was studied on the recovery efficiency of lead ions.

3. Results and discussion

3.1. Characterization of NONP

Fig. 1 shows the SEM, TEM, DLS and XRD results of the synthesized NONP. Based on the SEM image (Fig. 1(a)), the NONP sample contains mono-dispersive and highly crystalline agglomerated spherical nanoparticles with the average diameter of 35 nm. TEM micrographs (Fig. 1(b)) show uniform nanoparticles with the average diameter of 15 nm. Based on dynamic light scattering (DLS), the particle size distribution is in the range of 10–25 nm with an average diameter of 15 nm (Fig. 1(c)). The DLS result confirms that's of TEM analysis.

Fig. 1(d) shows XRD patterns of NONP sample. These patterns were used for the identification of the synthesized nanoparticles. The main diffraction peaks that were observed at 2θ = 37.3°, 43.3°, 63.18°, 75.3° and 79.5° indicate the formation of nickel oxide particles with high purity in face-centered cubic (FCC) crystalline structure [26]. The crystallite size of NiO nanoparticles can be estimated by the Debye–Scherrer equation (Eq. (3)) from the biggest diffraction peak of NiO nanoparticles [27].

$$D = \frac{0.94\,\lambda}{\beta \mathrm{Cos}\theta} \tag{3}$$

where λ is the wavelength of X-ray (0.154056 nm), β is the full width of the peak at half maximum height and θ is the peak position. The average size of NiO particles was calculated about 13 nm. This is in a good agreement with values observed by TEM and DLS studies (Fig. 1) which shows average size of 15 nm.

In chemical adsorption of metal ions, it is expected that some bands of sorbent areincurred blue or red shifts and one or more new bands is observed in wave numbers less than 1,000 cm^{-1} [28]. Fig. 2 shows the FTIR spectrums of NONP before and after treating with a lead ion solution. In Fig. 2(a), there are some characteristic bands at 596.89; 614.85; 1,629.9; 2,921.97; and 3,249.63 cm^{-1}. The band at 596.89 cm^{-1} reveals the presence of NiO. The band at 1,629.90 cm^{-1} represented that the sample contained a trace amount of water. The weak bands in the region of 1,000–1,500 cm^{-1} are assigned to the O–C=O symmetric and asymmetric stretching vibrations and the C–O is stretching vibration which indicated the adsorbed CO_2 and CO on NONP. The band at 3249.63 cm^{-1} is related

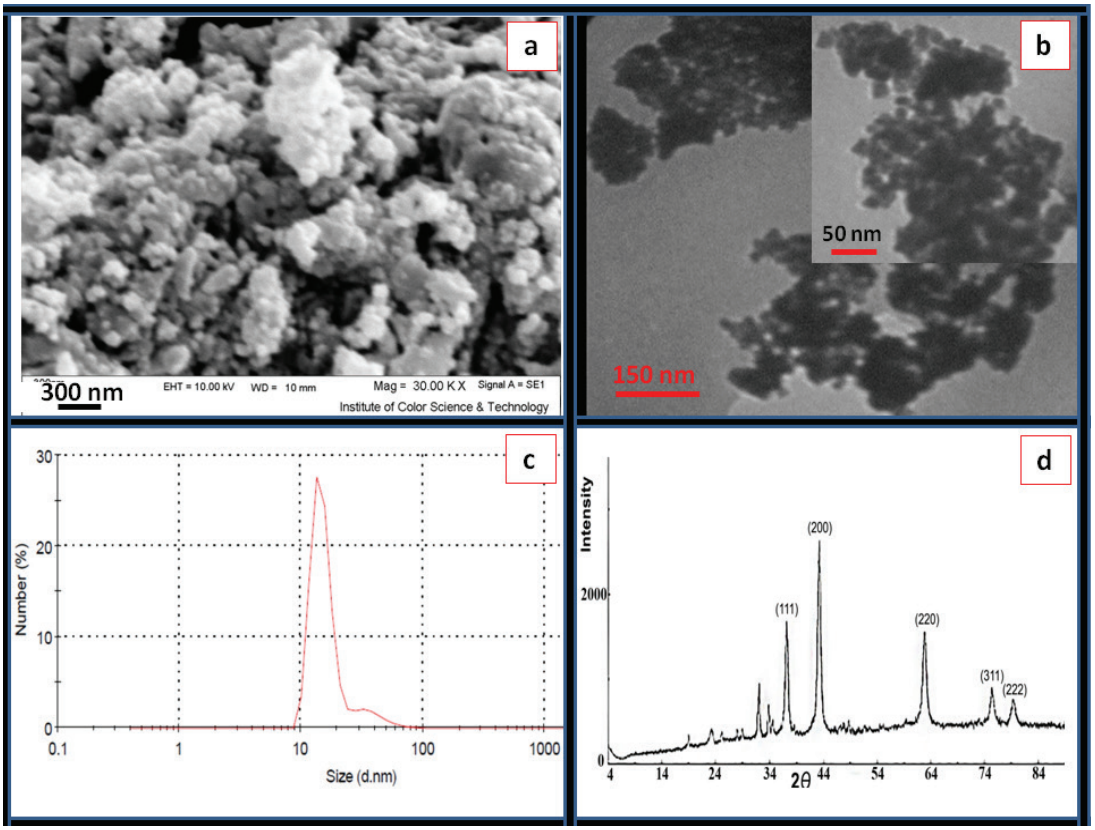

Fig. 1. (a) SEM image, (b) TEM micrograph, (c) DLS diagram and (d) XRD patters of the synthesized NONP.

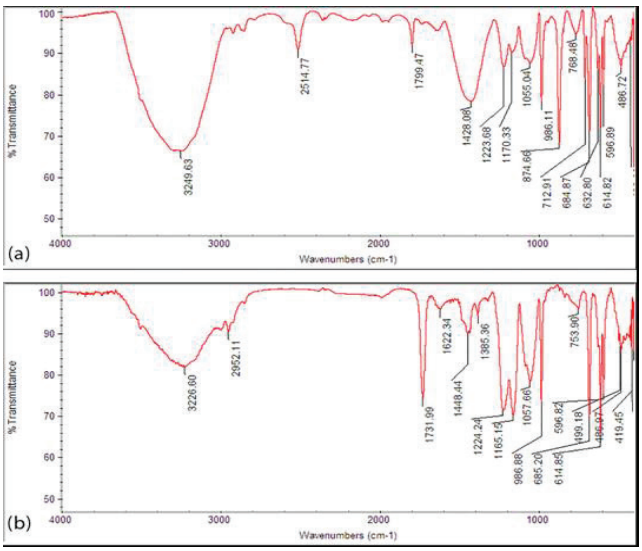

Fig. 2. FTIR spectrums NONP before (a) and after (b) treating with lead ion solution.

to the hydroxyl group. Therefore, the NONP in solution is hydrated. The height of hydroxyl band is strongly decreased after treating with lead ions because, hydroxyl groups chemically interact with lead ions. The bands in the range of 500–1,000 cm^{-1} are related to metal-O bonds.

3.2. Adsorption studies

The NiO nanoparticles were used a new and potential reuseable adsorbent for the removal of heaveay metal ions from the polluted water. The practical steps will be resecively explained.

3.2.1. Cation selection

Before starting the adsorption study, the ability of NONP for the adsorption of some heavy metal ions was separately investigated. Fig. 3 shows the removal efficiencies of some heavy metal ions by NONP. As it can be seen in Fig. 3, lead ions show the best removal efficiency. This result is because of the strong interaction between a soft acid (Pb^{2+}) and soft base (hydroxy group). In the followings, the sorption of lead ions on NONP will be fully investigated.

3.2.2. Time dependency of lead ion sorption on NONP and sorption kinetics

To investigate the effect of contact time on the sorption efficiency of lead ions on NONP, the removal values of lead ions by NONP are determined in the time range of 10–90 min for three different concentrations of lead ions (100, 200, 300 μg ml^{-1}: Fig. 4). As it can be seen in Fig. 4, the removal efficiency is increased when the contact time is increased. For all concentrations, the lead ion removal could be done before 60 min with an efficiency of 95% or more. The required time for the quantitative sorption of each ion depends on the sorption kinetics.

In order to examine the diffusion mechanism involved during the sorption process, two kinetic models were tested.

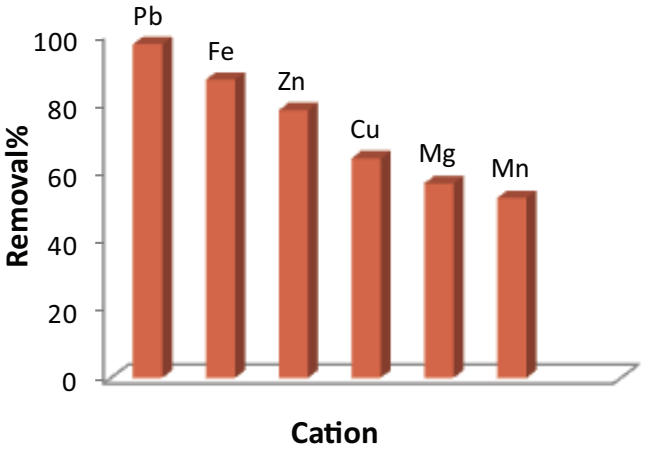

Fig. 3. Removal values for some heavy metal ion by NONP in separate solutions.

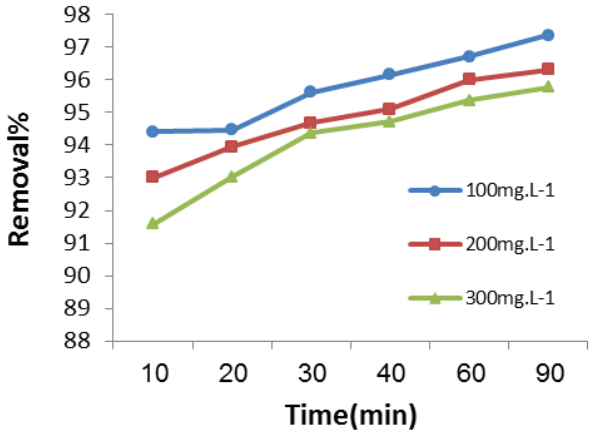

Fig. 4. Effect of contact time on the removal of Pb(II) by NiO adsorbent.

The adsorption data were firstly fitted to pseudo-first-order kinetic model, which is given by Eq. (4) [29]:

$$\log(q_e - q_t) = \log q_e - \frac{K_1}{2.303} t \tag{4}$$

where q_e and q_t are the amounts of adsorbent adsorbed (mg g^{-1}) at equilibrium and at contact time t (min), respectively, and k_1 is the pseudo-first-order rate constant (min^{-1}). The first-order-rate constant k_1 can be obtained from the slope of the plot ln $(q_e - q_t)$ vs. t (Fig. 5). Based on the obtained results, the R^2 values obtained are relatively small and the experimental q_e values do not agree with the values calculated from the linear plots. The results of these experiments were summarized in Table 1. In the next step, the data were examined by the pseudo-second-order kinetic model which is given by Eq. (5) [30]:

$$\frac{t}{q_t} = \frac{1}{k_2 q_e^2} + \frac{t}{q_e} \tag{5}$$

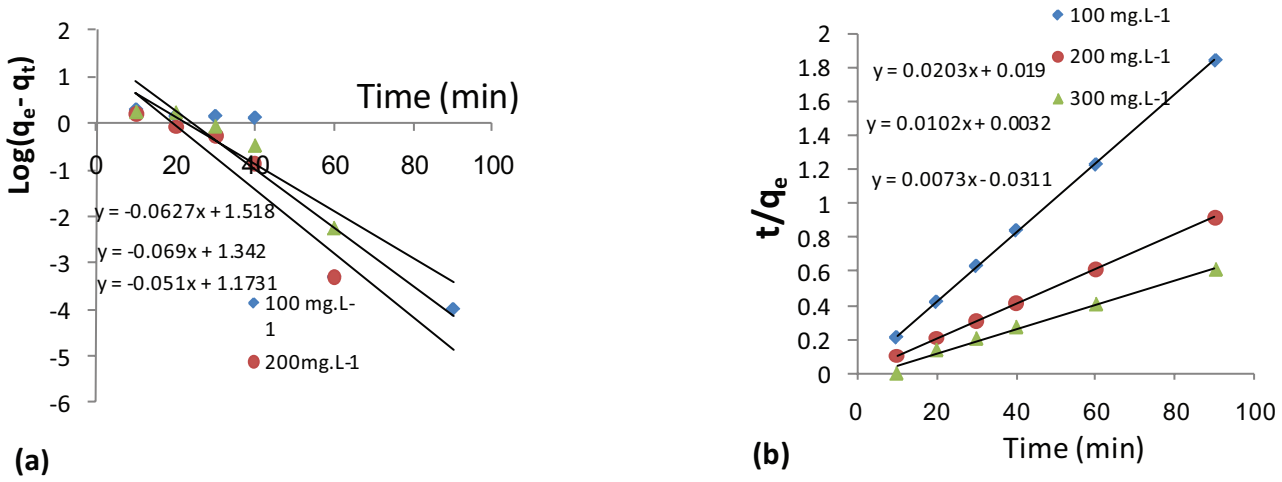

Fig. 5. Kinetic models of Pb (II) sorption by NiO, pseudo-first-order kinetics (a), pseudo-second-order kinetic (b).

Table 1
Pseudo-first-order kinetics and pseudo-second-order kinetics constants of lead ion sorption on NONP

Metal ions	C_0 (mg. g^{-1})	First-order kinetics		Second-order kinetics	
		K_1 (min^{-1})	R^2	K_2 ($gmg^{-1}min^{-1}$)	R^2
Pb(II)	100	0.6587	0.849	52.631	0.9998
	200	0.7451	0.8777	312.5	1
	300	0.8524	0.8737	32.154	1

Table 2
Adsorption isotherm parameters of lead ions on NiO nanoparticles

Isotherm model	Parameters	25°C	35°C	45°C
Langmuir	q_{max} (mgg^{-1})	50.7	48.423	47.981
	k_l (Lmg^{-1})	416.6	370.37	384.61
	R^2	0.9938	0.9875	0.9949
Freundlich	K_F (mg g^{-1}) (Lmg^{-1})$^{1/n}$	198.0659	186.475	167.248
	n	1.778	1.765	1.6299
	R^2	0.9261	0.8826	0.871
Temkin	A	9.6953	7.3545	6.5465
	B	104.51	113.27	116.88
	R^2	0.9721	0.9826	0.9817

where k_2 is the rate constant of pseudo-second-order adsorption (g mg^{-1} min^{-1}), q_e and q_t are the amounts adsorbed per unit mass at equilibrium and at any time t, respectively. Based on the experimental data of q, and t, the equilibrium sorption capacity (q_e) and the pseudo-second-order rate constant (k_2) can be determined from the slope and intercept of a plot of t/q, vs. t.

It was found that the pseudo-second-order model gives a satisfactory fit to all of the experimental data. The linear plots of sorption kinetics to the pseudo-second-order model and the calculated kinetic parameters are given in Fig. 5 and Table 1, respectively.

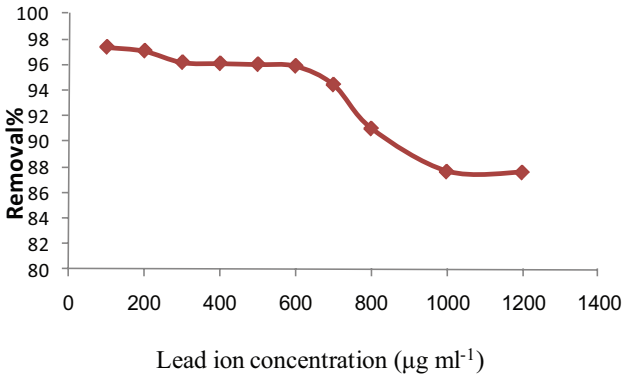

Fig. 6. Effects of initial concentration of lead ion on the removal efficiency.

3.2.3. Adsorption isotherms

The initial concentration of the analyte is an important parameter that could affect the absorption. To evaluate this factor, some solutions with concentrations of (100–1,200) µg ml^{-1} of lead ions were prepared with a pH of 5. In practice, 2.0 mg ml^{-1} nanoparticles were added to each of them and then were stirred for 60 min. After centrifuging, the residual concentration of lead ions was determined. Fig. 6 shows the results of these studies.

Adsorption capacity at different equilibrium concentrations can be described by the adsorption isotherms. Fig. 7 shows the adsorption isotherms for Pb (II) on NONP at pH 5.0 and different temperatures of 25°C, 35°C and 45°C. In this study, Langmuir, Freundlich and Temkin models were used to describe the experimental sorption data. The Langmuir model assumes a homogeneous surface of the

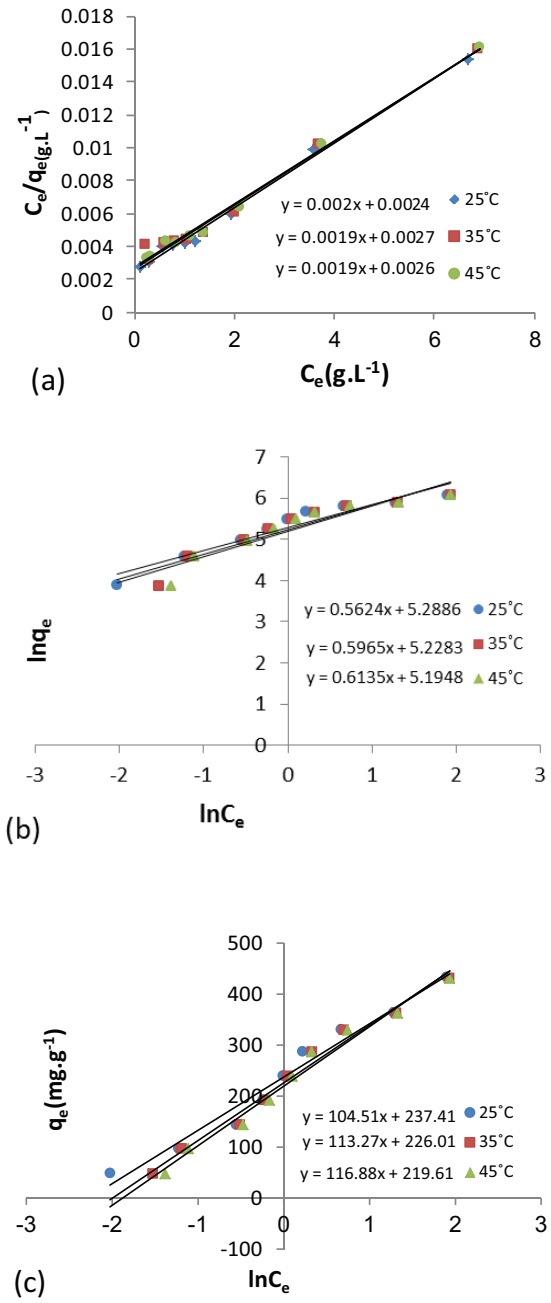

Fig. 7. Adsorption isotherms of Pb (II) onto of NiO adsorbent: (a) Langmuir, (b) Freundlich and (c) Temkin (c).

adsorbent, that there is no interaction between the adsorbed species on adjacent active sites and the sorption is localized in a monolayer. It is then assumed that once a molecule occupies a site, no further adsorption can take place at that site. Langmuir isotherm can be represented as [31]:

$$q_e = \frac{q_m b C_e}{1 + b C_e} \tag{6}$$

where C_e is the equilibrium concentration of Pb (II) in solution (μg ml^{-1}), q_e is the equilibrium capacity of Pb (II) on the adsorbent (mg g^{-1}), q_{max} is the maximum adsorption capacity of the adsorbent corresponding to complete monolayer coverage on the surface (mg g^{-1}), and b is the Langmuir adsorption constant (ml μg^{-1}) and related to the free energy of adsorption. Eq. (7) can be rearranged to a linear form as follows:

$$\frac{C_e}{q_e} = \frac{1}{b q_m} + \frac{C_e}{q_m} \tag{7}$$

where q_{max} and b can be calculated from the intercepts and the slopes of the linear plots of C_e/q_e vs. C_e.

The Freundlich isotherm can be given as follows:

$$q_e = k_f C_e^{1/n} \tag{8}$$

The linearized form of the Freundlich isotherm is given as:

$$\log q_e = \log k_f + \frac{1}{n} \log C_e \tag{9}$$

where q_e is the equilibrium adsorption capacity of the adsorbent in mg g^{-1}, C_e is the equilibrium concentration of heavy metal ions in ppm, K_f is the constant related to the adsorption capacity of the adsorbent in ppm, and n is the constant related to the adsorption intensity.

Temkin isotherm contains a factor that explicitly considers interactions between attraction and absorption capacities [32,33] and can be expressed as follows:

$$q_e = \frac{RT}{B} \ln(AC_e), \quad \frac{RT}{b} = B \tag{10}$$

A linear form of the Temkin isotherm would be as follows:

$$q_e = B \ln A + B \ln C_e \tag{11}$$

where q_e is the equilibrium adsorption capacity of the adsorbent in mg g^{-1}, C_e is the equilibrium concentration of heavy metal ions in ppm, A is the equivalent to the fixed link, linked with maximum energy (1 mg^{-1}). Constant B: (no units) is proportional to the heat of adsorption. b is the constant of Temkin isotherm (jmol^{-1}). The obtained results of three isotherms were shown in Table 2 and Fig. 7.

The obtained adsorption capacity was compared with those of the previous reports (Table 3). The presented data shows NONP revealed a big adsorption capacity for the removal of lead ions.

3.2.4. Effect of pH

The heavy metal ions adsorption is strongly pH dependent, and so the pH of the aqueous solution is an important controlling parameter in the heavy metal ions adsorption process [39]. The influence of initial pH on adsorption percentage was studied in the range of 2–7 for cations of Pb^{2+}, Zn^{2+}, Fe^{2+} and Cu^{2+}. The relationship between the initial pH values and the quantities of heavy metal ions removal efficiency was presented in Fig. 8(b). At pHs lower than 4, adsorption of

metal ions is less, because the proton concentration is higher than those of metal ions and such a situation was not favorable for metal ions removal. Therefore, the negative sites of the nickel oxide nanoparticles will be occupied by proton ions so that the metal ions adsorption will be decreased. To further disclose the adsorption mechanism between nickel oxide nanoparticles and heavy metal ions, the point of zero charge (pH_{PZC}) of nickel (II) oxide was conducted at different pH values (Fig. 8(b)). In Fig. 8(b), label of A refers to initial pH values of solution before mixing with NONP (pH_i) and label of B refers to the final pH of solution after mixing with NONP (pH_f). Based on the data in Fig. 8(b), the pH_{PZC} value of NONP was at pH 4.5 which concluded that the adsorbent surface had a positive and negative charges in pHs less than 4.5 and higher than 4.5, respectively.

3.2.5. Effect of dosage of adsorbent

The results of the experiments with varying adsorbent dosage are presented in Fig. 9. The presented data shows that an increase in the adsorbent dosage from 0.2 to 5 mg ml^{-1} causes the increase of the lead ion removal efficiency from 66% to 100%. In 100 μg ml^{-1} initial concentration of lead ions, 2 mg ml^{-1} NONP is enough to complete removal of lead ions.

Table 3
Comparison of monolayer maximum adsorption capacities of some adsorbents for Pb (II) from aqueous solution

Adsorbents	Maximum adsorption capacities (mg g^{-1})	References
Pb (II)-imprinted polymer in nano-TiO_2 matrix	22.7	[34]
MWCNTs/iron oxide	12	[35]
Multi-walled carbon nanotubes	<40	[36]
ZnO nano sheets	6.7	[37]
CeO_2 nano crystals	9.2	[38]
Nickel oxide nanoparticles	50.7	This study

3.2.6. Effect of temperature on the lead ion removal

The results of the experiments with varying temperature are presented in Fig. 10. A temperature-dependency increasing on removal value shows the lead ion adsorption on NONP could be an endothermic process in the temperature range of 5°C–25°C. The removal less at temperatures higher than 25°C shows that there is the different temperature-dependence of adsorption and desorption processes. At bigger temperatures than 25°C, temperature coefficient of desorption kinetics is more than that of adsorption.

3.2.7. Effect of sample volume

To investigate the effect of the initial sample volume, six experiments were done in different initial sample volumes while lead ion miles were same in all of them (Fig. 11). By increasing the volume of the solution from the 25 ml to 500 ml the removal value decreases from 100% to 67%. The observed results of lead ion removal imply that the sorption of lead ions on NONS is equilibrium process. For more clarification, the lead ion sorption can be shown in the following equations:

$$Pb^{2+}_{aq} + Site_{NONP} \Leftrightarrow Pb^{2+}.Site_{NONP} \quad (12)$$

$$K = \frac{\left[Pb^{2+}.Site_{NONP}\right]}{\left[Pb^{2+}_{aq}\right]\left[Site_{NONP}\right]} \quad (13)$$

where pb^{2+}_{aq} is lead ion in solution, $Site_{NONP}$ is the active site on NONP, $Pb^{2+}.Site_{NONP}$ is the occupied site via lead ions on

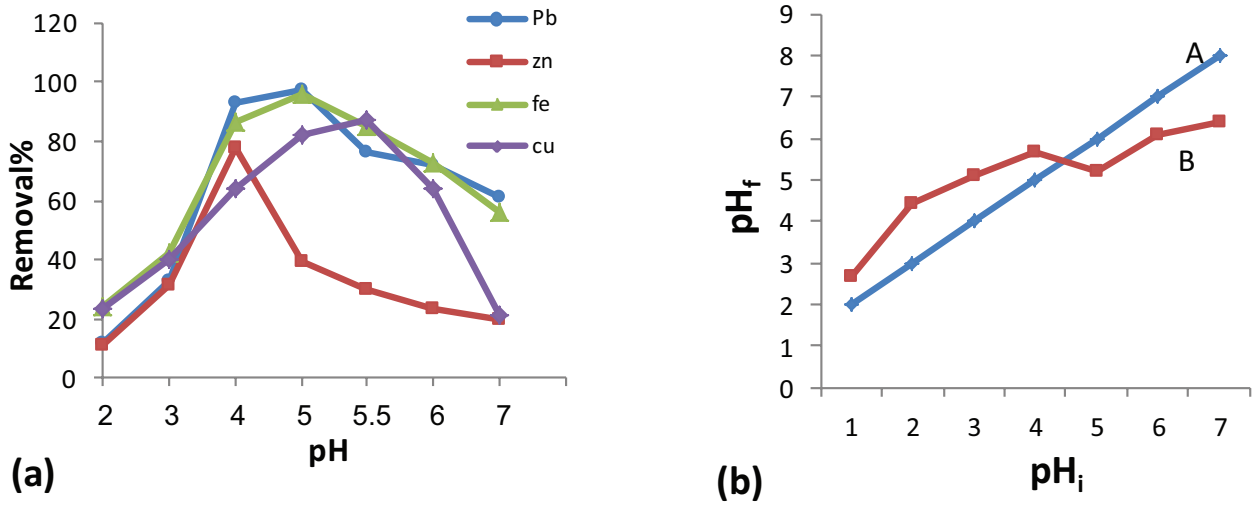

Fig. 8. (a) Effect of pH on the removal percentages of some heavy metal ions by NONP; (b) effect of adding NONP on changing pH for the determination of pH_{PZC} of NONP; (c) in all experiments, 50 ml lead ion solution with 100 μg ml^{-1} was mixed with 100 mg NONP for 1 h.

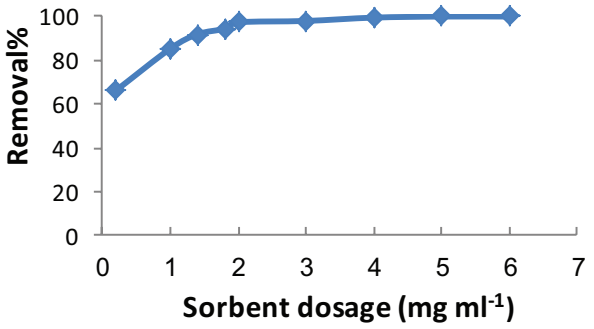

Fig. 9. Effect of dosage of adsorbent on the heavy metal ions removal efficiency by NiO adsorbent.

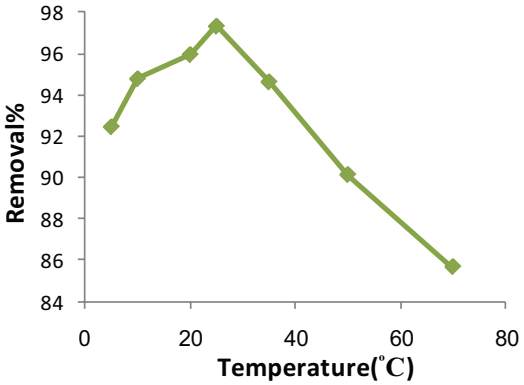

Fig. 10. Effect of temperature on the heavy metal ions removal efficiency by NiO adsorbent.

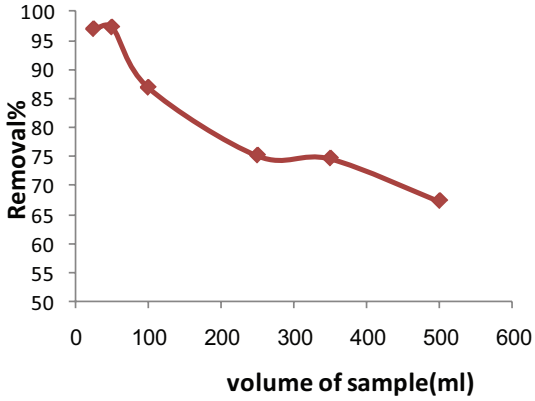

Fig. 11. Effect of initial sample volume on the heavy metal ions removal efficiency.

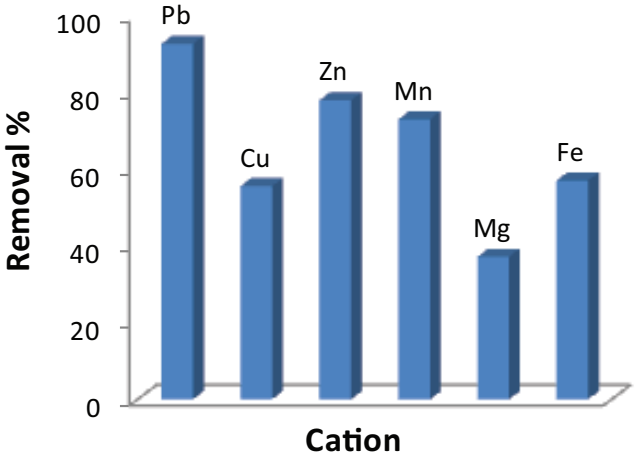

Fig. 12. Effect of the presence of other ions on the lead ion retention.

NONP and K is the equilibrium constant. In diluted solutions (initial volume bigger than 50 ml), the residual concentration (mole L^{-1}) is decreased. Therefore, to keep constant the equilibrium, much more lead ions should be free in solution.

3.2.8. Effect of the presence of other ions on the lead ion removal

The effects of other metal ions with different concentrations (5–800 ppm) on the lead ions removal were examined. The summary of the obtained results is shown in Table 4. The results show that the lead ion adsorption on NONP is a selective process and the presence of other metal ions does not have a significant interfering on lead ion removal.

3.2.9. Application of NONP for the removal of other heavy metal ions

In the optimized conditions for lead ions adsorption, the removal of some heavy metal ions by NONP were examined. Fig. 12 shows that NONP can be used as a selective and quantitative sorbent for the removal of lead ions from contaminated water but, the removal of other heavy metal ions are not analytically acceptable.

3.3. Thermodynamic study

The effect of temperature on an adsorption process depends on its mechanism. Temperature has two major effects on these processes. The first is the direct dependency

Table 4
Effect of other metal ions on lead ion removal

Concentration (ppm)	Cations							
	Pb^{2+}	Zn^{2+}	Na^{1+}	Mg^{2+}	Mn^{2+}	Cu^{2+}	Fe^{2+}	Al^{3+}
5	96.226	96.226	94.79	99.04	98.386	95.50	94.60	98.56
100	95.145	95.145	93.68	97.668	93.44	94.84	92.56	94.013
400	92.11	92.11	93.65	92.50	93.22	94.42	87.92	89.19
800	86.148	86.148	93.126	84.84	93.01	91.82	84.39	70.00

Table 5
Values of various thermodynamic parameters for adsorption of Pb(II) on NiO adsorbent

Adsorbent	ΔH° (kJ mol^{-1})	ΔS° (Jmol^{-1}K^{-1})	ΔG° (kJ mol^{-1})				
			283 K	298 K	308 K	323 K	343 K
NONP	–19.968	–28.959	–11.772	–11.338	–11.048	–10.614	–10.035

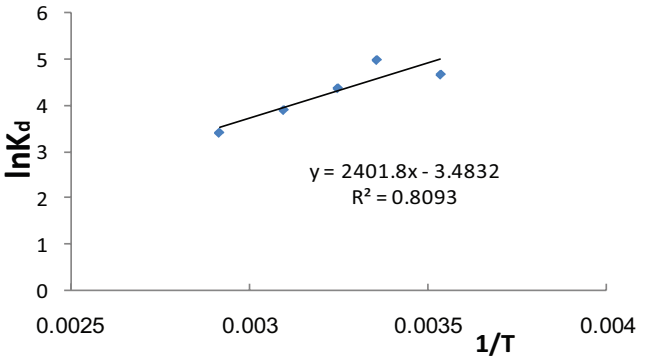

Fig. 13. Variation of equilibrium constant (K_d) as a function of temperature (1/T).

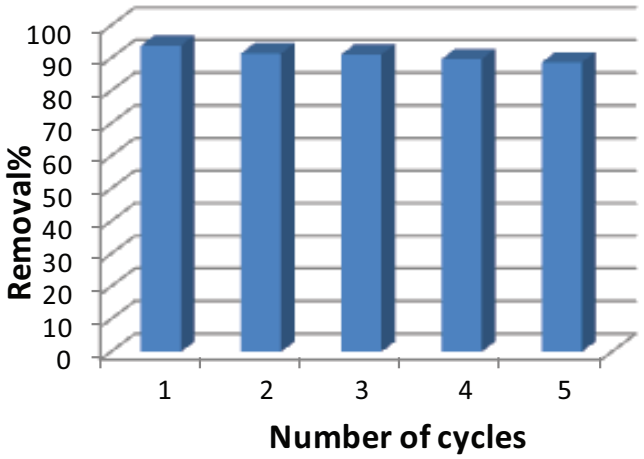

Fig. 14. Five consecutive adsorption of Pb (II) ions on NONP in regeneration studies.

of diffusion rate of the sorbate across the external boundary layer and in the internal pores of the adsorbents. The variation of equilibrium capacity of the sorbent towards sorbate is the second temperature effect in such processes [40,41].

To investigate the influence of temperature on the uptake of lead ions by the studied adsorbents, the removal of these ions (100 mg L^{-1}) from aqueous solution, adjusted at pH 5, by 100 mg of NONP sorbent was performed as a function of temperature in the range 283–343 K. The corresponding distribution coefficient (K_d) was calculated by Eq. (14):

$$K_d = \frac{(C_0 - C_e)}{C_e} \times \frac{V}{m} \quad (14)$$

where C_0 and C_e are initial and equilibrium concentrations of lead ions (mg L^{-1}), respectively, V is the volume of the aqueous phase solution (L) and m is the amount of adsorbent (g).

The Van't Hoff equation (Eq. (15)):

$$\ln K_d = -\frac{\Delta H^\circ}{RT} + \frac{\Delta S^\circ}{R} \quad (15)$$

conducts calculating enthalpy (ΔH°) and entropy changes (ΔS°), by analysis the lnK_d vs. T^{-1} plot (Fig. 13). The values of ΔH° and ΔS° were calculated from the slope and intercept of linear plot of lnK_d vs. T^{-1}, respectively [40]:

The Gibbs free energy changes (ΔG°), thus can be determined by Eq. (16):

$$\Delta G^\circ = \Delta H^\circ - T\Delta S^\circ \quad (16)$$

The calculated thermodynamic parameters for the adsorption process of lead ions on the adsorbent are given in Table 5.

The calculated thermodynamic parameters for the adsorption process of lead ions on the adsorbent are given in Table 5. In our study, the negative values of ΔH° confirmed the exothermic nature of the process. The negative ΔG° value indicated a spontaneous process.

3.4. Regeneration of NONP adsorbents

NONP loaded by Pb ions were washed with 4 ml 3 M HNO_3 and reused for the removal of lead ions. Fig. 14 shows five consecutive adsorptions of lead ions on NONP. During five sorption/desorption processes, the removal efficiency does not show a considerable loss (less than 5%).

4. Conclusions

The results of the current study illustrated that the sol-gel pyrrolysis method based on PVA as gel making agent is an applicable and inexpensive method for the synthesis of NiO nanoparticles. Based on TEM image, the mean particle size 15 nm was measured and confirmed those of XRD and DLS results. The NiO nanoparticles can be used as a suitable sorbent for the removal of Pb (II) ions from aqueous solutions at pH 5. The experimental data on lead ion adsorption on NiO nanoparticles was fitted to pseudo-second-order kinetic model and the Langmuir isotherm with the highest capacity of 50.7 mg g^{-1}. Finally, the experimental data showed that NiO nanoparticles can be reused as a recoverable sorbent for many times.

Acknowledgement

The authors would like to thank the financial support of this work by Abhar Payame Noor University Research Council.

References

[1] A.R. Ngomsik, A. Bee, J.M. Siaugue, D. Talbot, V. Cabuil, G. Cote, Co (II) removal by magnetic alginate beads containing Cyanex, J. Hazard. Mater., 166 (2009) 1043–1049.

[2] C. Gheorghiu, J. Cable, D.J. Marcogliese, M.E. Scott, Effects of waterborne zinc on reproduction, survival and morphometrics of *Gyrodactylus turnbulli* (Monogenea) on guppies (*Poecilia reticulata*), Int. J. Parasitol., 37 (2007) 375–381.

[3] M.M. Matlock, B.S. Howerton, D.A. Atwood, Chemical precipitation of heavy metals from acid mine drainage, Water. Res., 36 (2002) 4757–4764.

[4] M. Kiel, D. Dobslaw, K.H. Engesser, Comparison of biological and chemical treat-ment processes as cost-effective methods for elimination of benzoate in saline waste waters, Water. Res., 66 (2014) 1–11.

[5] I. Dobrevsk, M.D. Todorova, T. Panayotova, Electroplating rinse waste water treatment by ion exchange, Desalination, 108 (1997) 277–280.

[6] B. An, Q. Liang, D. Zhao, Removal of arsenic(V) from spent ion exchange brine using a new class of starch-bridges magnetite nanoparticles, Water. Res., 45 (2011) 1961–1972.

[7] M. Arulkumar, K. Thirumalai, P. Sathishkumar, T. Palvannan, Rapid removal of chromium from aqueous solution using novel prawn shell activated carbon, Chem. Eng. J., 185–196 (2012) 178–186.

[8] A.B. Albadarin, C. Mangwandi, A.H. Al-Muhtaseb, G.M. Walker, S.J. Allen, M.N.M. Ahmad, Kinetic and thermodynamics of chromium ions adsorption onto low-cost dolomite adsorbent, Chem. Eng. J., 179 (2012) 193–202.

[9] S.B. Wang, H.T. Li, Structure directed reversible adsorption of organic dye onmesoporous silica in aqueous solution, Micropor. Mesopor. Mater., 97 (2006) 21–26.

[10] A. Gil, F.C.C. Assis, S. Albeniz, S.A. Korili, Removal of dyes from wastewaters by adsorption on pillared clays, Chem. Eng. J., 168 (2011) 1032–1040.

[11] F.L. Fu, Q. Wang, Removal of heavy metal ions from wastewaters: a review, J. Environ. Manage., 92 (2011) 407–418.

[12] N. Galil, M. Rebhun, Primary chemical treatment minimizing dependence on bioprocess in small treatment plants, Water. Sci. Technol., 22 (1990) 203–210.

[13] B.J. Pan, B.C. Pan, W.M. Zhang, L. Lv, Q.X. Zhang, S.R. Zheng, Development of polymeric and polymer-based hybrid adsorbents for pollutants removal from waters, Chem. Eng. J., 151 (2009) 1929.

[14] S.P. Mishra, V.K. Singh, D. Tiwari, Radiotracer technique in adsorption study. Part XIV. Efficient removal of mercury from aqueous solutions by hydrous zirconium oxide, Appl. Radiat. Isot., 47 (1996) 15–21.

[15] C.A. Quirarte-Escalante, V. Soto, W. de la Cruz, G. Rangel Porras, R. Manríquez, S. Gomez-Salazar, Synthesis of hybrid adsorbents combining sol-gel processing and molecular imprinting applied to lead removal from aqueous streams, Chem. Mater., 21 (2009) 1439–1450.

[16] H.T. Fan, X.T. Sun, Z.G. Zhang, W.X. Li, Selective removal of lead(II) from aqueous solution by an ion-imprinted silica sorbent functionalized with chelating N-donor atoms, J. Chem. Eng., 59 (2014) 2106–2114.

[17] H.T. Fan, X.T. Sun, W.X. Li, Sol–gel derived ion-imprinted silica-supported organic–inorganic hybrid sorbent for selective removal of lead(II) from aqueous solution, J. Sol-Gel. Sci. Technol., 72 (2014) 144–155.

[18] D.P. Sui, H.X. Chen, L. Liu, M.X. Liu, C.C. Huang, H.T. Fan, Ion-imprinted silica adsorbent modified diffusive gradients in thin films technique: tool for speciation analysis of free lead species, Talanta, 148 (2016) 285–291.

[19] S. Babel, T.A. Kurniawan, Low-cost adsorbents for heavy metals uptake from contaminated water: a review, J. Hazard. Mater., 97 (2003) 219–243.

[20] T.A. Davis, B. Volesky, A. Mucci, A review of the biochemistry of heavy metal biosorption by brown algae, Water. Res., 37 (2003) 4311–4330.

[21] B. Viltužnik, A. Košak, Y.L. Zub, A. Lobnik, Removal of Pb(II) ions from aqueous systems using thiol-functionalized cobalt–ferrite magnetic nanoparticles, J. Sol-Gel. Sci. Technol., 68 (2013) 365–373.

[22] Y. Liu, Z. Liu, J. Gao, J. Dai, J. Han, Y. Wang, J. Xie, Y. Yan, Selective adsorption behavior of Pb(II) by mesoporous silica SBA-15-supported Pb(II)-imprinted polymer based on surface molecularly imprinting technique, J. Hazard. Mater., 186 (2011) 197–205.

[23] T. Mahmood, M.T. Saddique, A. Naeem, S. Mustafa, N. Zeb, K.H. Shah, M. Waseem, Kinetic and thermodynamic study of Cd(II), Co(II) and Zn(II) adsorption from aqueous solution by NiO, Chem. Eng. J., 171 (2011) 935–940.

[24] T. Sheela, Y.A. Nayaka, Kinetics and thermodynamics of nanoparticles, Chem. Eng. J., 191 (2012) 123–131.

[25] H. Karami, A. Aminifar, H. Tavallali, Z.A. Namdar, PVA-Based sol-gel synthesis and characterization of CdO–ZnO nanocomposite, J. Clust. Sci., 21 (2010) 1–9.

[26] J.V. Smith (Ed.), X-Ray Powder Data File, American Society for Testing Materials, 1960.

[27] G.U. Feng, S.F. Wang, M.K. Lu, G.J. Zhou, D. Xu, D.R. Yuan, Photoluminescence properties of SnO_2 nanoparticles synthesized by sol-gel method, J. Phys. Chem. B., 108 (2004) 8119–8123.

[28] R. Wang, Q. Li, D. Xie, H. Xiao, H. Lu, Synthesis of NiO using pine as template and adsorption performance for Pb(II) from aqueous solution, Appl. Sur. Sci., 279 (2013) 129–136.

[29] Y. Ho, Review of second-order models for adsorption systems, J. Hazard. Mater. B., 136 (2006) 681–689.

[30] B. Cheng, Y. Le, W. Cai, J. Yu, Synthesis of hierarchical $Ni(OH)_2$ and NiO nano sheets and their adsorption kinetics and isotherms to Congo Red in water, J. Hazard. Mater., 185 (2011) 889–897.

[31] S. Liang, X. Guo, N. Feng, Q. Tian, Adsorption of Cu^{2+} and Cd^{2+} from aqueous solution by mercator-acetic acid modified orange peel, Coll. Surf. B., 73 (2009) 10–14.

[32] M. Ozacar, I.A. Şengil, Adsorption of metal complex dyes from aqueous solutions by pine sawdust, Bioresour. Technol., 96 (2005) 791–195.

[33] I.D. Mall, V.C. Srivastava, N.K. Agarwall, I.M. Mishra, Removal of Congo Red from aqueous solution by bagasse fly ash and activated carbon: kinetic study and equilibrium isotherm analyses, Chemosphere., 61 (2005) 492–501.

[34] C. Li, J. Gao, J. Pan, Z. Zhang, Y. Yan, Synthesis, characterization, and adsorption performance of Pb(II)-imprinted polymer in nano-TiO_2 matrix, J. Environ. Sci., 21 (2009) 1722–1729.

[35] J. Hu, D. Shao, C. Chen, G. Sheng, J. Li, X. Wang, M. Nagatsu, Plasma-induced grafting of cyclodextrin onto multiwall carbon nanotube/iron oxides for adsorbent application, J. Phys. Chem. B., 114 (2010) 6779–6785.

[36] S. Yang, J. Hu, C. Chen, D. Shao, X. Wang, Mutual effects of Pb(II) and humic acid adsorption on multiwalled carbon nanotubes/polyacrylamide composites from aqueous solutions, Environ. Sci. Technol., 45 (2011) 3621–3627.

[37] X.F. Ma, Y.Q. Wang, M.J. Gao, H.Z. Xu, G.A. Li, A novel strategy to prepare ZnO/PbS heterostructured functional nanocomposite utilizing the surface adsorption property of ZnO Nano sheets, Catal. Today, 158 (2010) 459–463.

[38] C.Y. Cao, Z.M. Cui, C.Q. Chen, W.G. Song, W. Cai, Ceria hollow nanospheres produced by a template-free microwave-assisted hydrothermal method for heavy metal ion removal and catalysis, J. Phys. Chem. C, 114 (2010) 9865–9870.

[39] M. Yunus Pamukoglu, F. Kargi, Removal of copper(II) ions from aqueous medium by biosorption onto powdered waste sludge, Process Biochem., 41 (2006) 1047–1054.

[40] P. Sharma, R. Tomar, Synthesis and application of an analogue of mesolite for the removal of uranium(VI), thorium(IV), and europium(III) from aqueous waste, Micropor. Mesopor. Mater., 116 (2008) 641–652.

[41] S. Wang, Y. Boyjoo, A. Choueib, Z.H. Zhu, Removal of dyes from aqueous solution using fly ash and red mud, Water. Res., 39 (2005) 129–138.